Inorganica Chimica Acta 461 (2017) 57–63

Contents lists available at ScienceDirect

Inorganica Chimica Acta

journal homepage: www.elsevier.com/locate/ica

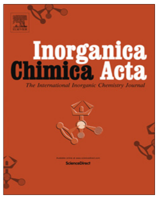

Research paper

Two- and three-dimensional silver acetylide frameworks with high-nuclearity silver cluster building blocks assembled using a bifunctional (4-ethynylphenyl)diphenyl phosphine ligand

Shaokang Zhang [a,1], Zongyao Zhang [b,1], Rui Cao [a,b,*]

[a] School of Chemistry and Chemical Engineering, Shaanxi Normal University, Xi'an 710119, China
[b] Department of Chemistry, Renmin University of China, Beijing 100872, China

ARTICLE INFO

Article history:
Received 7 October 2016
Received in revised form 15 December 2016
Accepted 10 January 2017

Keywords:
Bifunctional ligand
Silver acetylide
Coordination polymer
X-ray structure
Silver cluster

ABSTRACT

A bifunctional ligand precursor (4-ethynylphenyl)diphenyl phosphine was synthesized and used for constructing silver acetylide frameworks. Its reaction with Ag(I) in the presence of triethylamine afforded silver acetylide $[Ag\mathbf{L}]_n$, in which $\mathbf{L} = Ph_2P\text{-}C_6H_4\text{-}4\text{-}C{\equiv}C^-$ could act as a bifunctional ligand bearing both phenylethynide and phosphine binding sites for Ag(I). Reactions of $[Ag\mathbf{L}]_n$ and $AgCF_3CO_2$ under different conditions gave four silver acetylides. They are $[Ag_{18}\mathbf{L}_8(CF_3COO)_6(HCO_3)_4(DMF)_4]_n$ (**1**, DMF = dimethylformamide), $[Ag_{20}\mathbf{L}_8(CF_3COO)_{12}(DMF)_6]_n$ (**2**), $[Ag_{17}\mathbf{L}_6(CF_3COO)_9(HCO_3)_2]_n$ (**3**), and $[Ag_{17}\mathbf{L}_6(CF_3COO)_{9.58}(HCO_3)_{1.42}]_n$ (**4**). Crystallographic studies revealed that complex **1** crystallized in the triclinic space group $P\bar{1}$ with $a = 14.1252(9)$ Å, $b = 18.6012(12)$ Å, $c = 25.2137(17)$ Å, $\alpha = 108.340(2)°$, $\beta = 95.386(2)°$, $\gamma = 95.535(2)°$, $V = 6204.6(7)$ Å^3, and $Z = 1$. Complex **2** crystallized in the monoclinic space group $C2/c$ with $a = 48.046(4)$ Å, $b = 14.1860(10)$ Å, $c = 34.943(2)$ Å, $\beta = 98.315(3)°$, $V = 23{,}566(3)$ Å^3, and $Z = 4$. Complex **3** crystallized in the triclinic space group $P\bar{1}$ with $a = 15.5690(7)$ Å, $b = 16.7707(8)$ Å, $c = 34.0810(16)$ Å, $\alpha = 93.4040(10)°$, $\beta = 100.3690(10)°$, $\gamma = 94.8250(10)°$, $V = 8697.1(7)$ Å^3, and $Z = 2$. Complex **4** crystallized in the triclinic space group $P\bar{1}$ with $a = 15.5396(6)$ Å, $b = 16.7595(7)$ Å, $c = 34.0225(15)$ Å, $\alpha = 93.8140(10)°$, $\beta = 100.1000(10)°$, $\gamma = 94.9770(10)°$, $V = 8660.2(6)$ Å^3, and $Z = 2$. The presence of Ag(I)–ethynide, Ag(I)–P and Ag(I)–Ag(I) bonding interactions makes all four silver acetylides to have two- and three-dimensional framework structures with unusual high-nuclearity silver cluster building blocks.

1. Introduction

Silver acetylides have attracted continuous attention because of their intrinsic and fundamental importance in structural [1–6] and photophysical chemistry [7–12], and also their potential applications in organic transformation [13–17], catalysis [18–22], and material sciences [23–26]. Extensive efforts have resulted in the synthesis and structural characterization of many silver acetylides, from which diverse Ag(I)–ethynide coordination modes and metallophilic [27] Ag(I)–Ag(I) interactions have been demonstrated [1–5,28–39]. However, unmodified silver acetylides usually aggregate to form organometallic polymers [6], which are not soluble and precipitate immediately upon formation. As a result, in the synthesis of these complexes, phosphine ligands, which have simple but strong Ag(I)–P coordination interactions, have been frequently used as capping ligands to confine the silver cluster to a certain size by preventing its uncontrolled and infinite growth [8,9,12,40–45].

Ligand design therefore plays a critical role in the research of silver acetylides. In addition to simple ligands containing one ethynide or one phosphine binding site for Ag(I), alkynyl ligands that have two or more ethynide groups [31,32,37–39,46–49] and also di- and triphosphine ligands [9,12,40–42] have been explored for the construction of silver acetylides with various complicated structures largely due to the presence of additional coordination and bridging modes. However, silver acetylides reported so far in general present either discrete cluster structures [1–4,33,36] or polymeric structures with small silver cluster building blocks [6,31,34,35,37,46,48–50]. In order to make new silver acetylides with more structural diversities, we are interested in combining the benefits of both ethynide and phosphine binding sites in one single ligand. The resulted bifunctional ligand can use the ethynide

---

[*] Corresponding author at: School of Chemistry and Chemical Engineering, Shaanxi Normal University, Xi'an 710119, China.

E-mail address: ruicao@ruc.edu.cn (R. Cao).

[1] These authors contributed equally to this work.

http://dx.doi.org/10.1016/j.ica.2017.01.030
0020-1693/

part to create silver clusters and use the phosphine part to control the silver cluster size. Importantly, unlike using individual alkynyl and phosphine ligands, the assembly of both binding sites in one single ligand is expected to form silver acetylide frameworks through bridging Ag(I)–P-C_6H_4-4-C≡C–Ag(I) linkages.

Herein we report the design of (4-ethynylphenyl)diphenyl phosphine as a ligand precursor and its uses in the synthesis and assembly of silver acetylides. Upon deprotonation of the acetylene unit, the resulted bifunctional Ph_2P-C_6H_4-4-C≡C^- (**L**) ligand can interact with Ag(I) through both ethynide and phosphine coordination sites. Four silver acetylide complexes were isolated and structurally characterized, including $[Ag_{18}\mathbf{L}_8(CF_3COO)_6(HCO_3)_4(DMF)_4]_n$ (**1**, DMF = dimethylformamide), $[Ag_{20}\mathbf{L}_8(CF_3COO)_{12}(DMF)_6]_n$ (**2**), $[Ag_{17}\mathbf{L}_6(CF_3COO)_9(HCO_3)_2]_n$ (**3**), and $[Ag_{17}\mathbf{L}_6(CF_3COO)_{9.58}(HCO_3)_{1.42}]_n$ (**4**). Crystallographic studies showed that all four complexes represented very rare examples of silver acetylide frameworks assembled using high-nuclearity silver cluster building blocks. Complexes **1** and **2** have two-dimensional (2D) framework structures, while complexes **3** and **4** have three-dimensional (3D) framework structures.

2. Experimental section

2.1. Materials and methods

All reagents and solvents used were commercially available and were used as received. Triethylamine and dichloromethane were distilled with calcium hydride, tetrahydrofuran was distilled with sodium strips. Manipulations of air- and moisture-sensitive materials were performed under nitrogen gas using the standard Schlenk line technique. ^1H (400.0 MHz), ^{13}C (100.0 MHz) and ^{31}P (121.4 MHz, with proton decoupling) NMR spectra were recorded on a Brüker spectrometer operating at 400 MHz. Elemental analyses were carried out with Vario EL III elemental analyzer. FT-IR spectra were recorded with KBr pellets using a Bruker Tensor 27 spectrometer. Ligand precursor Ph_2P-C_6H_4-4-C≡CH was prepared using a modified method reported previously [51].

2.2. Preparation of 4-bromo-(trimethylsilylethynyl)benzene

To an anhydrous triethylamine solution (30 mL), 4-iodo-bromobenzene (2.0 g, 7.07 mmol) was dissolved at room temperature. This solution was cooled in an ice bath, and $Pd(PPh_3)_4$ (0.20 g, 0.18 mmol) and CuI (34.28 mg, 0.18 mmol) were added. Cold trimethylsilylacetylene solution (1.1 mL, 0.76 g, 7.78 mmol) was then added in a dropwise manner. The mixture was stirred in an ice bath for 1.5 h, and then saturated NH_4Cl aqueous solution (30 mL) was added. The product was extracted with CH_2Cl_2 (3 × 50 mL), and the organic phases were combined and dried over Na_2SO_4. Purification by chromatography on silica gel gave a white solid (1.73 g, 6.82 mmol, 96% yield). ^1H NMR ($CDCl_3$): δ 7.45–7.41 (m, 2H), 7.33–7.30 (m, 2H), 0.25 (s, 9H).

2.3. Preparation of Ph_2P-C_6H_4-4-C≡C-$SiMe_3$

To an anhydrous THF solution (50 mL), 4-bromo-(trimethylsilylethynyl)benzene (2.0 g, 7.9 mmol) was dissolved, and *n*-BuLi (2.5 M, 3.16 mL, 7.9 mmol) was added under nitrogen at −78 °C. The solution was stirred for 2 h before chlorodiphenylphosphine (1.82 g, 8.23 mmol) was added. The reaction mixture was stirred for an additional 2 h, and then the solvent was removed by rotary evaporator under a reduced pressure. The residue was purified by silica gel chromatography to afford a white powder (1.91 g, 5.33 mmol, 67% yield) ^1H NMR ($CDCl_3$): δ 7.42–7.16 (m, 14H), 0.22 (s, 9H). ^{31}P NMR ($CDCl_3$): δ −4.6 (s).

2.4. Preparation of Ph_2P-C_6H_4-4-C≡CH

To a methanol (80 mL) and dichloromethane (10 mL) solution of Ph_2P-C_6H_4-4-C≡C-$SiMe_3$ (0.95 g, 2.66 mmol), was added K_2CO_3 (0.74 g, 5.33 mmol). The suspension was stirred at room temperature for 2 h, and was then filtered. The crude product was purified by silica gel chromatography to give a white solid (0.75 g, 2.61 mmol, 98% yield) ^1H NMR ($CDCl_3$): δ 7.48–7.20 (m, 14H), 3.11 (s, 1H). ^{13}C NMR ($CDCl_3$): δ 138.91, 136.72, 133.93, 133.46, 132.11, 129.08, 128.74, 122.42, 83.49, 78.38. ^{31}P NMR ($CDCl_3$): δ −4.8 (s).

2.5. Preparation of $[Ag\mathbf{L}]_n$

Silver nitrate (67.95 mg, 0.4 mmol) was dissolved in acetonitrile (8 mL). Triethylamine (40.48 mg, 0.4 mmol) and Ph_2P-C_6H_4-4-C≡CH (0.11 g mg, 0.4 mmol) were added under stirring. The reaction mixture was stirred for 2 d in the dark to give a white precipitate, which was collected by filtration. The product was then washed by acetonitrile (3 × 3 mL), dried in vacuo and was used without further purification. Yield: 63.2% (99.43 mg).

2.6. Preparation of **1**

Complex $[Ag\mathbf{L}]_n$ (19.66 mg, 0.05 mmol) was dissolved in the solution of $AgCF_3CO_2$ (44.18 mg, 0.2 mmol) in DMF (3 mL). The reaction mixture was stirred overnight in the dark, and was filtered to give a clear yellow solution. Slow vapor diffusion using diethyl ether/petroleum ether (v/v = 1/1) afforded colorless crystalline plates of complex **1** in about 80% yield. Anal. Calcd. for $C_{188}H_{140}Ag_{18}F_{18}N_4O_{28}P_8$: C 41.55, H 2.60, N 1.03; found: C 41.72, H 2.76, N 0.90.

2.7. Preparation of **2**

Complex $[Ag\mathbf{L}]_n$ (19.66 mg, 0.05 mmol) was dissolved in the solution of $AgCF_3CO_2$ (16.57 mg, 0.075 mmol) in DMF (3 mL). The reaction mixture was stirred overnight in the dark, and was filtered to give a clear yellow solution. Slow vapor diffusion using diethyl ether afforded colorless crystalline plates of complex **2** in about 78% yield. Anal. Calcd. for $C_{202}H_{154}Ag_{20}F_{36}N_6O_{30}P_8$: C 38.92, H 2.49, N 1.35; found: C 40.17, H 2.68, N 1.21.

2.8. Preparation of **3**

Complex $[Ag\mathbf{L}]_n$ (19.66 mg, 0.05 mmol) was dissolved in the solution of $AgCF_3CO_2$ (49.70 mg, 0.225 mmol) in THF (3 mL). The reaction mixture was stirred overnight in the dark, and was filtered to give a clear yellow solution. Slow vapor diffusion using diethyl ether/*n*-hexane (v/v = 1/1) afforded yellow crystalline prisms of complex **3** in about 85% yield. Anal. Calcd. for $C_{140}H_{84}Ag_{17}F_{27}O_{28}P_6$: C 35.42, H 1.78; found: C 35.69, H 1.91.

2.9. Preparation of **4**

Complex $[Ag\mathbf{L}]_n$ (19.66 mg, 0.05 mmol) was dissolved in the solution of $AgCF_3CO_2$ (33.13 mg, 0.15 mmol) in THF (3 mL). The reaction mixture was stirred overnight in the dark, and was filtered to give a clear yellow solution. Slow vapor diffusion using diethyl ether/*n*-hexane (v/v = 1/1) afforded yellow crystalline prisms of complex **4** in about 75% yield. Anal. Calcd. for $C_{140.58}H_{84}Ag_{17}F_{28.74}O_{26.42}P_6$: C 35.46, H 1.78; found: C 35.63, H 1.89.

CAUTION! *Silver acetylide complexes are potentially explosive and should be handled with care and in small amounts.*

2.10. X-ray diffraction studies

Complete data for complexes **1**–**4** were collected. Single crystals suitable for X-ray analysis were each coated with Paratone-N oil, suspended in a small fiber loop, and placed in a cooled gas stream on a Bruker D8 QUEST X-ray diffractometer. Diffraction intensities were measured using graphite monochromated Mo Kα radiation (λ = 0.71073 Å) at 153(2) K and a combination of φ and ω scans. Data collection, indexing, data reduction, final unit cell refinements and absorption corrections were carried out using APEX2 [52]. Absorption corrections were applied using the program SADABS [53]. All structures were solved with direct methods using SHELXS [54] and refined against F^2 on all data by full-matrix least-squares with SHELXL [55], following established refinement strategies.

In the structures of **1**–**4**, all non-hydrogen atoms were anisotropically refined. All hydrogen atoms binding to carbon were included into the model at geometrically calculated positions and refined using a riding model. The isotropic displacement parameters of all hydrogen atoms were fixed to 1.2 times the U value of the atoms they are linked to (1.5 times for methyl groups). Details of the data quality and a summary of the residual values of the refinements are listed in Table 1. Automatic structure evaluation performed with PLATON as implemented in the CheckCIF routine resulted in one level A alert concerning solvent accessible voids for all four structures. Because of the framework structures of **1**–**4**, there are large spaces in their crystal structures. Therefore, it is reasonable to have large solvent accessible voids in their crystal X-ray structures.

3. Results and discussion

3.1. Synthesis of complexes 1–4

Ligand precursor Ph_2P-C_6H_4-4-C≡CH was made according to the synthetic route shown in Scheme S1. Br-C_6H_4-4-C≡C-$SiMe_3$ reacted with *n*-BuLi at −78 °C, and then Ph_2PCl was added dropwisely to give the coupling product Ph_2P-C_6H_4-4-C≡C-$SiMe_3$. Subsequent deprotection of the trimethylsilyl group using K_2CO_3 gave the desired bifunctional ligand precursor bearing both acetylene and phosphine moieties. The reaction of Ph_2P-C_6H_4-4-C≡CH and $AgNO_3$ in the presence of triethylamine afforded silver acetylide $[Ag\mathbf{L}]_n$ polymers, which were not soluble in acetonitrile and precipitated immediately as white powders upon formation. This product was collected by filtration, washed carefully by acetonitrile and was dried in vacuo before the use in subsequent synthesis.

The reaction of $[Ag\mathbf{L}]_n$ and 4 equivalents of $AgCF_3CO_2$ in DMF resulted in a clear yellow solution. Slow vapor diffusion of diethyl ether/petroleum ether (v/v = 1/1) into the resulted DMF solution afforded colorless crystalline plates of complex **1** in 5 d. The use of a mixture of diethyl ether/petroleum ether was aimed to slow down the vapor diffusion rate of diethyl ether, because the use of pure diethyl ether caused the rapid precipitation. Similarly, the reaction of $[Ag\mathbf{L}]_n$ and 1.5 equivalents of $AgCF_3CO_2$ in DMF gave complex **2**. If the same reaction between $[Ag\mathbf{L}]_n$ and $AgCF_3CO_2$ was conducted in tetrahydrofuran instead of DMF, the products were **3** and **4** with the starting molar ratio of $[Ag\mathbf{L}]_n$: $AgCF_3CO_2$ = 1: 4.5 and 1:3, respectively. All four complexes were isolated in moderate yields (75–85%), and were structurally characterized by the single crystal X-ray diffraction method.

3.2. Crystallographic studies of complex 1

Complex **1** crystallized in the triclinic space group $P\bar{1}$ with *a* = 14.1252(9) Å, *b* = 18.6012(12) Å, *c* = 25.2137(17) Å, α = 108.340(2)°, β = 95.386(2)°, γ = 95.535(2)°, *V* = 6204.6(7) Å^3, and *Z* = 1 (Table 1). As shown in Fig. 1, complex **1** contains a Ag_{14} cluster, which is located at the special position with a crystallographically required inversion center. The Ag(I)–Ag(I) bond distances are in the range of 2.8713(10) to 3.3329(11) Å, indicating the interactions between these d^{10} Ag(I) ions [6,56]. The Ag_{14} cluster can be viewed

Table 1
Crystal data and structure refinement parameters for complexes **1**–**4**.

Complex	**1**	**2**	**3**	**4**
Molecular formula	$C_{188}H_{140}Ag_{18}F_{18}N_4O_{28}P_8$	$C_{202}H_{154}Ag_{20}F_{36}N_6O_{30}P_8$	$C_{140}H_{84}Ag_{17}F_{27}O_{28}P_6$	$C_{140.58}H_{84}Ag_{17}F_{28.74}O_{26.42}P_6$
Formula wt. (g mol^{-1})	5434.46	6234.46	4746.68	4761.33
Temperature (K)	153(2)	153(2)	153(2)	153(2)
Radiation (λ, Å)	0.71073	0.71073	0.71073	0.71073
Crystal system	Triclinic	Monoclinic	Triclinic	Triclinic
Space group	$P\bar{1}$	C2/*c*	$P\bar{1}$	$P\bar{1}$
a (Å)	14.1252(9)	48.046(4)	15.5690(7)	15.5396(6)
b (Å)	18.6012(12)	14.1860(10)	16.7707(8)	16.7595(7)
c (Å)	25.2137(17)	34.943(2)	34.0810(16)	34.0225(15)
α (°)	108.340(2)	90	93.4040(10)	93.8140(10)
β (°)	95.386(2)	98.315(3)	100.3690(10)	100.1000(10)
γ (°)	95.535(2)	90	94.8250(10)	94.9770(10)
Volume (Å^3)	6204.6(7)	23,566(3)	8697.1(7)	8660.2(6)
Z	1	4	2	2
ρ_{calcd} (g cm^{-3})	1.454	1.757	1.813	1.826
μ (mm^{-1})	1.501	1.763	2.009	2.018
F(000)	2648	12,128	4560	4573
Crystal size (mm^3)	0.15 × 0.10 × 0.05	0.15 × 0.05 × 0.05	0.20 × 0.20 × 0.10	0.20 × 0.20 × 0.10
Theta range	1.99 to 26.54°	2.068 to 26.556°	2.093 to 26.462°	2.10 to 26.45°
Reflections collected	140,641	97,580	181,843	158,809
Independent reflections	25,598 [R(int) = 0.1134]	24,429 [R(int) = 0.0690]	35,809 [R(int) = 0.0328]	35,611 [R(int) = 0.0353]
Completeness	99.1%	99.9%	99.9%	99.7%
Goof	0.721	0.846	0.875	0.840
Final R indices	R1[a] = 0.0741	R1[a] = 0.0529	R1[a] = 0.0573	R1[a] = 0.0537
[R > 2σ (I)]	*w*R$_2$[b] = 0.1927	*w*R$_2$[b] = 0.1242	*w*R$_2$[b] = 0.1561	*w*R$_2$[b] = 0.1481
R indices (all data)	R1[a] = 0.1243	R1[a] = 0.0946	R1[a] = 0.0759	R1[a] = 0.0740
	*w*R$_2$[b] = 0.2250	*w*R$_2$[b] = 0.1461	*w*R$_2$[b] = 0.1702	*w*R$_2$[b] = 0.1602
Largest diff. peak and hole (e Å^{-3})	4.295 and −3.073	1.369 and −1.443	3.596 and −2.950	3.352 and −2.876

[a] $R_1 = \Sigma||F_o| - |F_c||/|F_o|$.
[b] $wR_2 = (\Sigma[w(F_o^2 - F_c^2)^2]/\Sigma[w(F_o^2)^2])^{0.5}$.

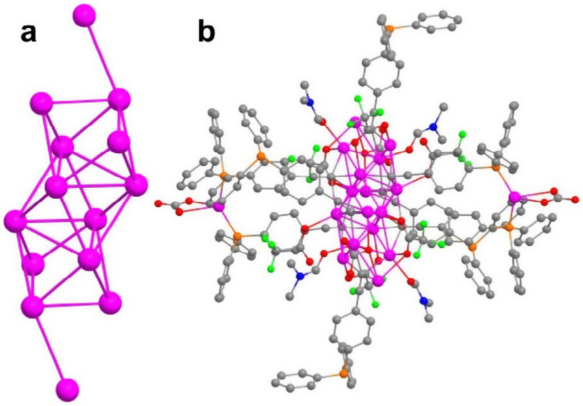

Fig. 1. (a) The Ag_{14} cluster core of complex **1**. (b) Ball-and-stick representation of the repeating unit of **1**. All hydrogen atoms are omitted for clarity. Color code: pink, silver; gray, carbon; orange, phosphorus; green, fluorine; red, oxygen; blue, nitrogen. (For interpretation of the references to colour in this figure legend, the reader is referred to the web version of this article.)

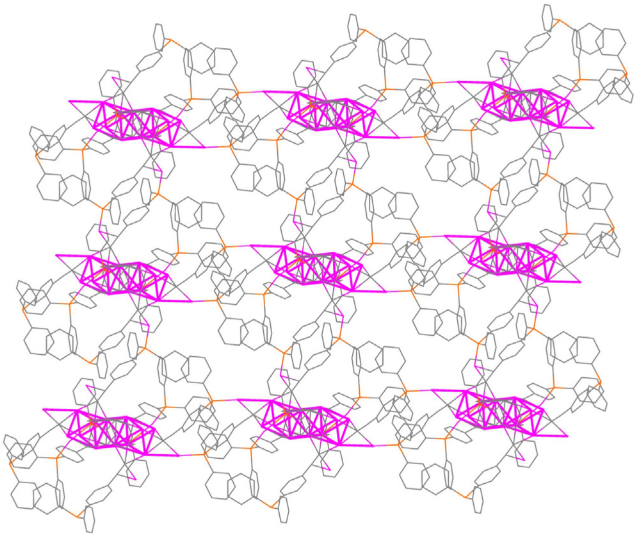

Fig. 3. The 2D plane network viewed along *c* axis in the X-ray structure of **1**, showing the Ag_{14} cluster building blocks. All hydrogen atoms, CF_3COO^- and HCO_3^- anions and DMF groups are omitted for clarity.

as the stacking of four Ag_3 triangles with two additional Ag(I) atoms each located at one end of the core structure (Fig. 1a). The Ag_{14} cluster is bound and stabilized by eight ethynide ligands (two C1≡C2, two C21≡C22, two C41≡C42, and two C61≡C62), six CF_3COO^- and two HCO_3^- anions, and four coordinating DMF solvent molecules. The two Ag7 atoms at the end of the core each are further bound to the P2 atom of a phosphine ligand, whose ethynide moiety binds to another Ag_{14} cluster. This P2 atom is expected to act as the capping ligand to prevent the uncontrolled and infinite growth of the silver cluster. The Ag7–P2 bond length is found to be 2.393(3) Å. It is worth noting that the carbonate groups found in the X-ray structure of **1** are likely due to the fixation of carbon dioxide from air, which is similar to previous results of synthesizing silver acetylides [1].

In addition to this Ag_{14} cluster, two symmetry equivalent Ag8 atoms are found to be each coordinated by two phosphine ligands through Ag8–P3 (2.442(6) Å) and Ag8–P4 (2.455(5) Å) interactions (Fig. 1b). Each Ag8 atom is coordinated by an additional HCO_3^- anion through Ag8–O9 and Ag8–O10 interactions. Interestingly, two symmetry equivalent Ag9 atoms each are connected to the Ag_{14} cluster through the coordination with the C1≡C2 ethynide group through π bond interactions (Ag9–C1 2.307(9) Å and Ag9–C2 2.566(11) Å) and the oxygen atoms from one CF_3COO^- group (O3) and one HCO_3^- group (O12). The relatively long Ag9–Ag1 (3.3201(10) Å) and Ag9–Ag3 (3.2929(10) Å) bonds indicate the presence of weak interactions between the Ag9 atom and the Ag_{14} cluster. The Ag9 atom is further bound to the P1 atom of a phosphine ligand, whose ethynide moiety binds to another Ag_{14} cluster, with an Ag9–P1 bond length of 2.383(3) Å. Importantly, the interactions of Ag9–P1 (Fig. 2a, along *a* axis) and Ag7–P2 (Fig. 2b, along *b* axis) bonds extend the molecular structure to a 2D polymeric structure with high-nuclearity Ag_{14} clusters acting as the building blocks (Fig. 3). Based on these results, the formula of complex **1** can be determined to be $[Ag_{18}\mathbf{L}_8(CF_3COO)_6(HCO_3)_4(DMF)_4]_n$ (the thermal ellipsoid plot of the X-ray structure of **1** is depicted in Fig. S1).

3.3. Crystallographic studies of complex 2

Complex **2** crystallized in the monoclinic space group C2/*c* with $a = 48.046(4)$ Å, $b = 14.1860(10)$ Å, $c = 34.943(2)$ Å, $\beta = 98.315(3)°$, $V = 23{,}566(3)$ Å^3, and $Z = 4$ (Table 1). Complex **2** contains a Ag_{16} cluster, which is located at the special position with a crystallographically required inversion center (Fig. 4). This Ag_{16} cluster is similar to the Ag_{14} cluster represented in the structure of **1**. It can be viewed as the stacking of four Ag_3 triangles with two Ag (I) atoms each located at one end of the core and with two additional Ag(I) atoms each located at the flank of the core (Fig. 4a). The Ag(I)–Ag(I) bond distances are in the range of 2.8867(7) to 3.2139(7) Å. This Ag_{16} cluster is bound and stabilized by eight ethynide ligands (two C1═C2, two C21═C22, two C41═C42, and two C61═C62), eight CF_3COO^- anions and four coordinating DMF solvent molecules. The two Ag6 atoms at the end of the core each are bound to the P1 atom of a phosphine ligand, whose ethynide moiety binds to another Ag_{16} cluster, with a Ag6–P1 bond length of 2.3923(19) Å. The two Ag8 atoms at the flank of the core each are bound to the P2 atom of a phosphine ligand, whose ethynide

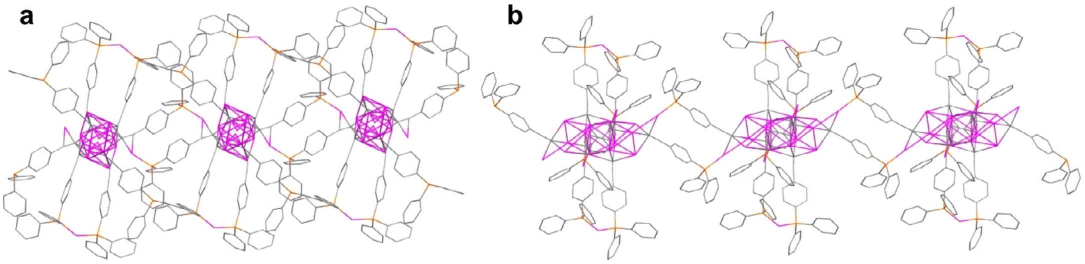

Fig. 2. (a) The 1D chain along *a* axis in the X-ray structure of **1**. (b) The 1D chain along *b* axis in the X-ray structure of **1**. All hydrogen atoms, CF_3COO^- and HCO_3^- anions and DMF groups are omitted for clarity.

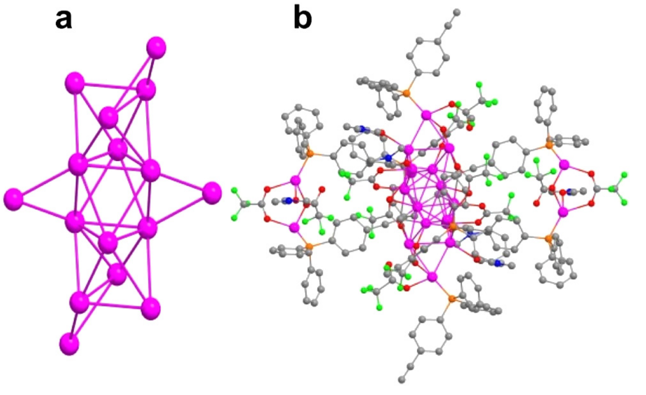

Fig. 4. (a) The Ag_{16} cluster core of complex **2**. (b) Ball-and-stick representation of the repeating unit of **2**. All hydrogen atoms are omitted for clarity. Color code: pink, silver; gray, carbon; orange, phosphorus; green, fluorine; red, oxygen; blue, nitrogen. (For interpretation of the references to colour in this figure legend, the reader is referred to the web version of this article.)

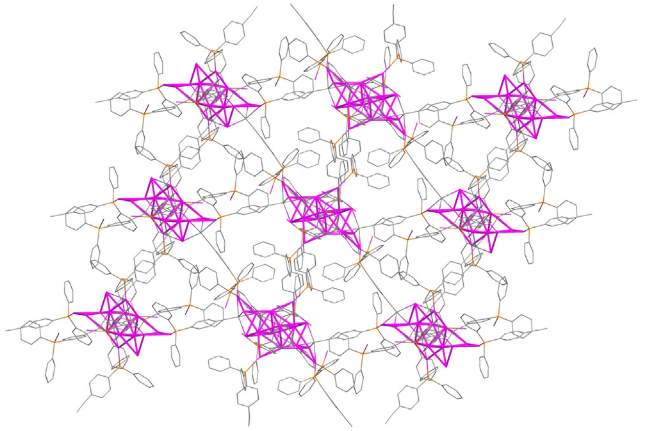

Fig. 6. The 2D plane network viewed along *a* axis in the X-ray structure of **2**, showing the Ag_{16} cluster building blocks. All hydrogen atoms, CF_3COO^- anions and DMF groups are omitted for clarity.

moiety also binds to another Ag_{16} cluster, with a Ag8–P2 bond length of 2.4186(17) Å. As a consequence, these phosphine ligands are found to act as capping ligands to confine the silver cluster to a certain size.

In addition to the Ag_{16} cluster, two symmetry equivalent Ag_2 units were found to be flanked by two phosphine ligands of P3 and P4 in the X-ray structure of **2** (Fig. 4b). The Ag9–P3 bond length is 2.354(2) Å, while the Ag10–P4 bond length is 2.358(2) Å. These two Ag(I) atoms are linked together by two CF_3COO^- anions. One CF_3COO^- anion bridges Ag9 and Ag10 through two O atoms, while the other CF_3COO^- anion bridges the two Ag(I) atoms through one O atom. Ag9 is coordinated by an additional DMF solvent molecule. These results give complex **2** the formula of $[Ag_{20}\mathbf{L}_8(CF_3COO)_{12}(DMF)_6]_n$ (the thermal ellipsoid plot of the X-ray structure of **2** is depicted in Fig. S2). Similar to complex **1**, in the structure of **2**, the interactions of Ag8–P2 (Fig. 5a, along *b* axis) and Ag6–P1 (Fig. 5b, along *c* axis) bonds extend the molecular structure to a 2D polymeric structure with high-nuclearity Ag_{16} clusters acting as the building blocks (Fig. 6).

3.4. Crystallographic studies of complexes **3** and **4**

Complex **3** crystallized in the triclinic space group $P\bar{1}$ with $a = 15.5690(7)$ Å, $b = 16.7707(8)$ Å, $c = 34.0810(16)$ Å, $\alpha = 93.4040(10)°$, $\beta = 100.3690(10)°$, $\gamma = 94.8250(10)°$, $V = 8697.1(7)$ Å^3, and $Z = 2$ (Table 1). Complex **3** contains a Ag_{15} cluster, which is located at the general position without any crystallographically required symmetry elements. The Ag(I)–Ag(I) bond distances are in the range of 2.8598(8) to 3.3436(7) Å. The Ag_{15} cluster can be viewed as two Ag_7 caps linked by a central Ag6 atom (Fig. 7a). The Ag_{15} cluster is bound and stabilized by six ethynide ligands ($C1{\equiv}C2$, $C21{\equiv}C22$, $C41{\equiv}C42$, $C61{\equiv}C62$, $C81{\equiv}C82$ and $C101{\equiv}C102$), nine CF_3COO^- and two HCO_3^- anions. The four Ag(I) atoms located at the end of the Ag_{15} cluster core each are bound to a phosphine ligand with Ag12–P3 bond length at 2.3869(19) Å, Ag13–P4 bond length at 2.3958(19) Å, Ag14–P1 bond length at 2.3888(17) Å, and Ag15–P2 bond length at 2.3972(18) Å. All these phosphine ligands have their ethynide moieties bound to other Ag_{15} clusters. Similar to complex **1**, the carbonate groups found in the X-ray structure of **3** are likely due to the fixation of carbon dioxide from air during the synthesis. For the two carbonate groups, one bridges three Ag(I) atoms, while the other bridges two Ag(I) atoms.

In addition to the Ag_{15} cluster, two Ag(I) atoms, Ag16 and Ag17, are found in the X-ray structure of **3** and play significant roles in constructing the polymeric structure (Fig. 7b). For Ag16, it is connected to the Ag_{15} cluster through the binding with three CF_3COO^- anions (O4, O6 and O7), and is further bound to the P5 atom of a phosphine ligand with a Ag16–P5 bond length at 2.3488(18) Å. For Ag17, it is connected to the Ag_{15} cluster through the binding with two CF_3COO^- anions (O14 and O18), and is further bound to the P6 atom of a phosphine ligand with a Ag17–P6 bond length at 2.342(2) Å. The formula of complex **3** can be then determined to be $[Ag_{17}\mathbf{L}_6(CF_3COO)_9(HCO_3)_2]_n$ (the thermal ellipsoid plot of the X-ray structure of **3** is depicted in Fig. S3).

Significantly, the many bridging interactions of $Ag(I){-}P{-}C_6H_4{-}4{-}C{\equiv}C{-}Ag(I)$ in the structure of **3** extend the molecular structure to a 3D polymeric structure with 1D chains (Fig. 8), 2D planes (Fig. 9) and 3D structures (Fig. 10) presented. The use of a Ag_{15} cluster as the building block for the assembly of such a 3D organometallic polymer is unprecedented.

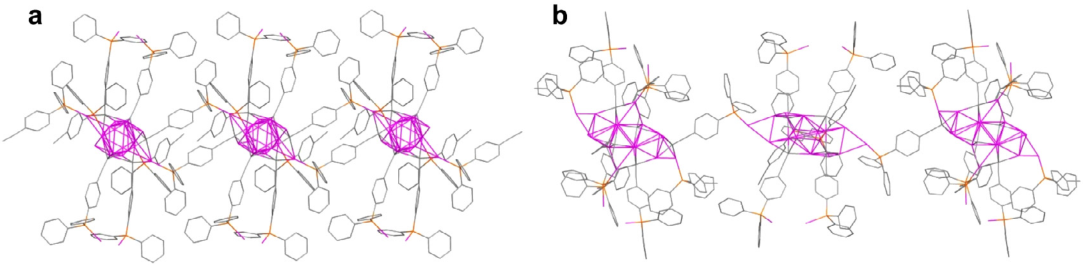

Fig. 5. (a) The 1D chain along *b* axis in the X-ray structure of **2**. (b) The 1D chain along *c* axis in the X-ray structure of **2**. All hydrogen atoms, CF_3COO^- anions and DMF groups are omitted for clarity.

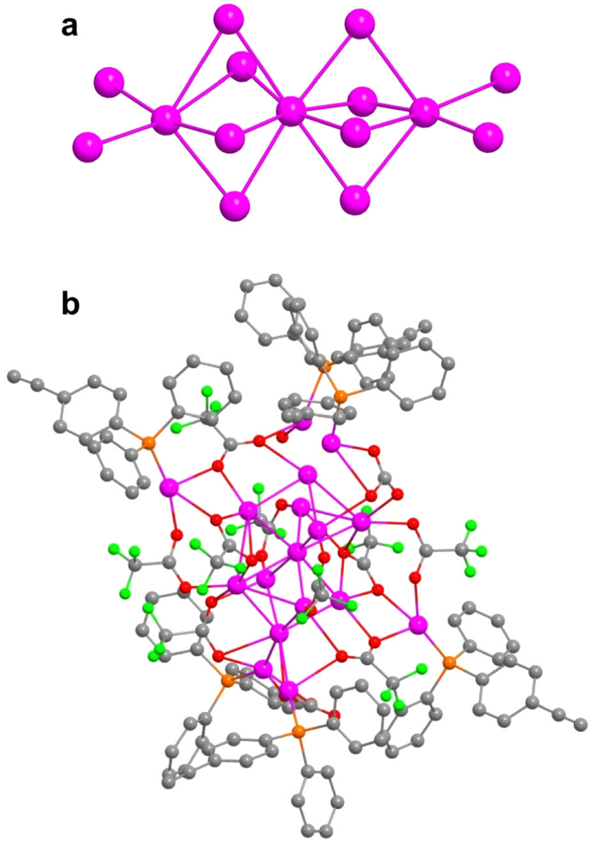

Fig. 7. (a) The Ag_{15} cluster core of complex **3**. (b) Ball-and-stick representation of the repeating unit of **3**. All hydrogen atoms are omitted for clarity. Color code: pink, silver; gray, carbon; orange, phosphorus; green, fluorine; red, oxygen. (For interpretation of the references to colour in this figure legend, the reader is referred to the web version of this article.)

The structure of complex **4** is almost identical to that of **3**. Complex **4** crystallized in the triclinic space group $P\bar{1}$ with a = 15.5396 (6) Å, b = 16.7595(7) Å, c = 34.0225(15) Å, α = 93.8140(10)°, β = 100.1000(10)°, γ = 94.9770(10)°, V = 8660.2(6) $Å^3$, and Z = 2 (Table 1). In the structure of **4**, the carbonate group that bridges three Ag(I) atoms is partially replaced by a CF_3COO^- anion. Free structural refinement gave a ratio of 58% CF_3COO^- and 42% HCO_3^- anions at this position. Except this difference, the structures of complexes **3** and **4** are the same. The formula of complex **4** is $[Ag_{17}\mathbf{L}_6(CF_3COO)_{9.58}(HCO_3)_{1.42}]_n$ (the thermal ellipsoid plot of the X-ray structure of **4** is depicted in Fig. S4). It is necessary to note that due to their structural similarities, it is possible that the bulk sample we isolated may be a mixture of **3** and **4**.

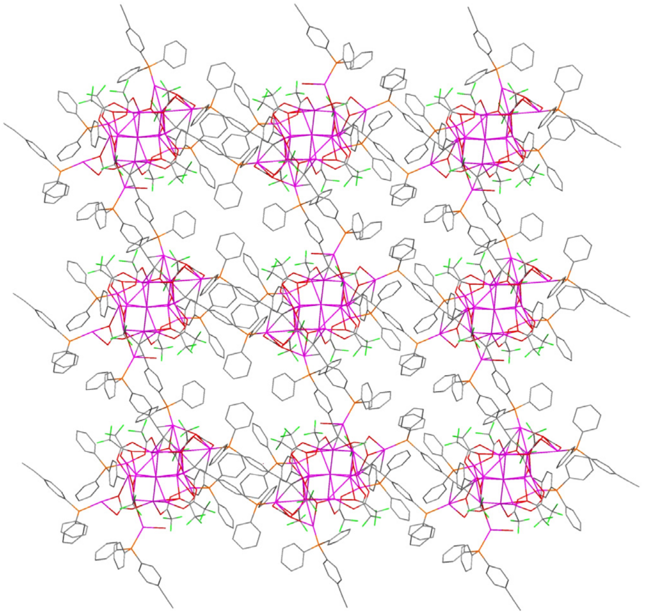

Fig. 9. The 2D plane network viewed along a axis in the X-ray structure of **3**, showing the Ag_{15} cluster building blocks. All hydrogen atoms are omitted for clarity.

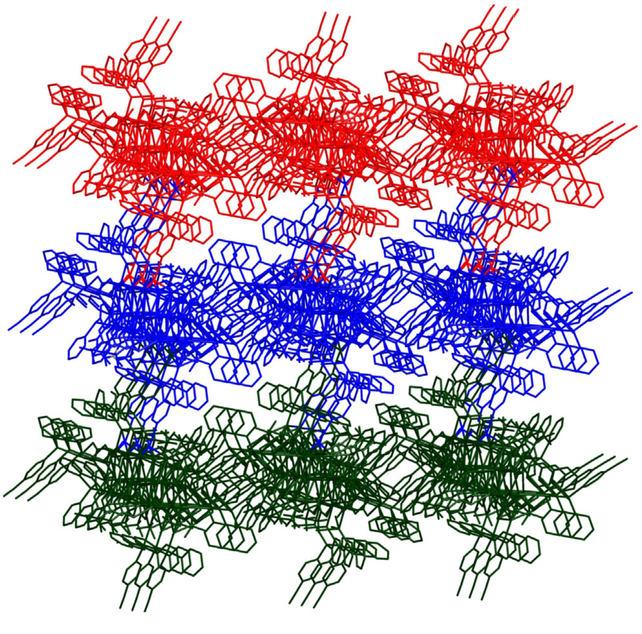

Fig. 10. The 3D framework in the X-ray structure of **3**, which is composed by the stacking of 2D planes. All hydrogen atoms are omitted for clarity.

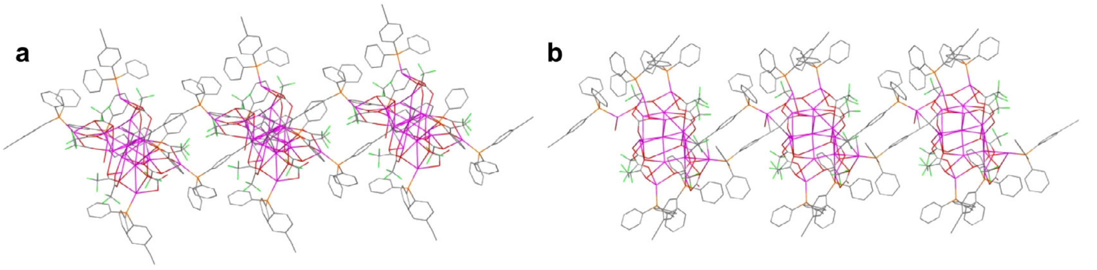

Fig. 8. (a) The 1D chain along a axis in the X-ray structure of **3**. (b) The 1D chain along b axis in the X-ray structure of **3**. All hydrogen atoms are omitted for clarity.

4. Conclusion

In conclusion, we designed and synthesized (4-ethynylphenyl) diphenyl phosphine. Its deprotonation gives the desired bifunctional ligand **L** = $Ph_2P\text{-}C_6H_4\text{-}4\text{-}C{\equiv}C^-$ bearing both phenylethynide and phosphine binding sites for Ag(I). With the use of this ligand, we were able to synthesize and structurally characterize four silver acetylides **1**–**4**. Complexes **1** and **2** have 2D polymeric structures, while complexes **3** and **4** have 3D structures. Ligand **L** plays significant roles in constructing these polymeric silver acetylides: (1) The ethynide moiety binds with Ag(I) atoms through both σ and π bonding interactions and is crucial for the formation of high-nuclearity silver clusters. (2) The phosphine ligand acts as capping ligands to confine the silver cluster to a certain size by preventing its uncontrolled and infinite growth. (3) The bridging Ag(I)–P-C_6H_4-4-C≡C–Ag(I) linkage extends molecular structures to polymeric structures. Complexes **1**–**4** represent unprecedented silver acetylide frameworks with high-nuclearity silver cluster building blocks.

Notes

The authors declare no competing financial interest.

Acknowledgments

We are grateful for support from the "Thousand Talents Program" of China, the National Natural Science Foundation of China (Grant No. 21101170 and 21573139), the Fundamental Research Funds for the Central Universities, and the Research Funds of Shaanxi Normal University.

Appendix A. Supplementary data

Scheme S1; Figures S1–S5; Crystallographic data as CIF for complexes **1**–**4**. Supplementary data associated with this article can be found, in the online version, at http://dx.doi.org/10.1016/j.ica.2017.01.030.

References

[1] S.D. Bian, J.H. Jia, Q.M. Wang, J. Am. Chem. Soc. 131 (2009) 3422–3423.
[2] J. Qiao, K. Shi, Q.M. Wang, Angew. Chem. Int. Ed. 49 (2010) 1765–1767.
[3] Y.P. Xie, T.C.W. Mak, Angew. Chem. Int. Ed. 51 (2012) 8783–8786.
[4] S.C.K. Hau, P.S. Cheng, T.C.W. Mak, J. Am. Chem. Soc. 134 (2012) 2922–2925.
[5] F. Gruber, M. Jansen, Angew. Chem. Int. Ed. 49 (2010) 4924–4926.
[6] X. Liu, Q.L. Yi, Y.Z. Han, Z.N. Liang, C.H. Shen, Z.Y. Zhou, J.L. Sun, Y.Z. Li, W.B. Du, R. Cao, Angew. Chem. Int. Ed. 54 (2015) 1846–1850.
[7] V.W.W. Yam, K.K.W. Lo, K.M.C. Wong, J. Organomet. Chem. 578 (1999) 3–30.
[8] M.C. Blanco, J. Cámara, M.C. Gimeno, A. Laguna, S.L. James, M.C. Lagunas, M.D. Villacampa, Angew. Chem. Int. Ed. 51 (2012) 9777–9779.
[9] I.O. Koshevoy, A.J. Karttunen, I.S. Kritchenkou, D.V. Krupenya, S.I. Selivanov, A. S. Melnikov, S.P. Tunik, M. Haukka, T.A. Pakkanen, Inorg. Chem. 52 (2013) 3663–3673.
[10] R. Zhang, C.Y. Zhao, X.M. Li, Z.Y. Zhang, X.C. Ai, H. Chen, R. Cao, Dalton Trans. 45 (2016) 12772–12778.
[11] T.L. Zhang, Y.J. Hu, J.X. Kong, X.G. Meng, X.M. Dai, H.B. Song, CrystEngComm 12 (2010) 3027–3032.
[12] Y. Jiang, Y.T. Wang, Z.G. Ma, Z.H. Li, Q.H. Wei, G.N. Chen, Organometallics 32 (2013) 4919–4926.
[13] U. Halbes-Letinois, J.M. Weibel, P. Pale, Chem. Soc. Rev. 36 (2007) 759–769.
[14] J.M. Weibel, A. Blanc, P. Pale, Chem. Rev. 108 (2008) 3149–3173.
[15] D. Tejedor, S. López-Tosco, F. Cruz-Acosta, G. Méndez-Abt, F. García-Tellado, Angew. Chem. Int. Ed. 48 (2009) 2090–2098.
[16] Y. Unoh, K. Hirano, T. Satoh, M. Miura, Angew. Chem. Int. Ed. 52 (2013) 12975–12979.
[17] J. Ke, C. He, H.Y. Liu, M.J. Li, A.W. Lei, Chem. Commun. 49 (2013) 7549–7551.
[18] Y. Yamamoto, Chem. Rev. 108 (2008) 3199–3222.
[19] G.C. Fang, X.H. Bi, Chem. Soc. Rev. 44 (2015) 8124–8173.
[20] J.Q. Liu, Z.X. Fang, Q. Zhang, Q. Liu, X.H. Bi, Angew. Chem. Int. Ed. 52 (2013) 6953–6957.
[21] M. Gao, C. He, H.Y. Chen, R.P. Bai, B. Cheng, A.W. Lei, Angew. Chem. Int. Ed. 52 (2013) 6958–6961.
[22] J.Q. Liu, Z.H. Liu, N.N. Wu, P.Q. Liao, X.H. Bi, Chem. Eur. J. 20 (2014) 2154–2158.
[23] J. Nishijo, O. Oishi, K. Judai, N. Nishi, Chem. Mater. 19 (2007) 4627–4629.
[24] B.K. Teo, Y.H. Xu, B.Y. Zhong, Y.K. He, H.Y. Chen, W. Qian, Y.J. Deng, Y.H. Zou, Inorg. Chem. 40 (2001) 6794–6801.
[25] H.S. Lo, E.C.C. Cheng, H.L. Xu, W.H. Lam, N.Y. Zhu, V.K.M. Au, V.W.W. Yam, J. Organomet. Chem. 812 (2016) 43–50.
[26] Z.Y. Zhang, Y. Yang, H.Y. Sun, R. Cao, Inorg. Chim. Acta 434 (2015) 158–171.
[27] R. Zhang, Z.N. Liang, A.L. Han, H.T. Wu, P.W. Du, W.Z. Lai, R. Cao, CrystEngComm 16 (2014) 5531–5542.
[28] T.C.W. Mak, X.L. Zhao, Q.M. Wang, G.C. Guo, Coord. Chem. Rev. 251 (2007) 2311–2333.
[29] Q.M. Wang, Y.M. Lin, K.G. Liu, Acc. Chem. Res. 48 (2015) 1570–1579.
[30] L. Zhao, W.Y. Wong, T.C.W. Mak, Chem. Eur. J. 12 (2006) 4865–4872.
[31] L. Zhao, T.C.W. Mak, J. Am. Chem. Soc. 127 (2005) 14966–14967.
[32] L. Zhao, T.C.W. Mak, J. Am. Chem. Soc. 126 (2004) 6852–6853.
[33] Y.P. Xie, T.C.W. Mak, J. Am. Chem. Soc. 133 (2011) 3760–3763.
[34] L. Zhao, X.L. Zhao, T.C.W. Mak, Chem. Eur. J. 13 (2007) 5927–5936.
[35] L. Zhao, C.Q. Wan, J. Han, X.D. Chen, T.C.W. Mak, Chem. Eur. J. 14 (2008) 10437–10444.
[36] R. Zhang, X. Hao, X.M. Li, Z.Y. Zhou, J.L. Sun, R. Cao, Cryst. Growth Des. 15 (2015) 2505–2513.
[37] Z.F. Zhang, B. Li, X.G. Meng, X.B. Yin, T.L. Zhang, Dalton Trans. 42 (2013) 4306–4312.
[38] S.C.K. Hau, T.C.W. Mak, Cryst. Growth Des. 14 (2014) 3567–3575.
[39] S.C.K. Hau, T.C.W. Mak, Chem. Eur. J. 19 (2013) 5387–5400.
[40] I.O. Koshevoy, A.J. Karttunen, J.R. Shakirova, A.S. Melnikov, M. Haukka, S.P. Tunik, T.A. Pakkanen, Angew. Chem. Int. Ed. 49 (2010) 8864–8866.
[41] L.J. Xu, J.Y. Wang, L.Y. Zhang, L.X. Shi, Z.N. Chen, Organometallics 32 (2013) 5402–5408.
[42] I.O. Koshevoy, Y.C. Lin, A.J. Karttunen, M. Haukka, P.T. Chou, S.P. Tunik, T.A. Pakkanen, Chem. Commun. (2009) 2860–2862.
[43] I.O. Koshevoy, C.L. Lin, A.J. Karttunen, J. Jänis, M. Haukka, S.P. Tunik, P.T. Chou, T.A. Pakkanen, Inorg. Chem. 50 (2011) 2395–2403.
[44] I.O. Koshevoy, A.J. Karttunen, S.P. Tunik, M. Haukka, S.I. Selivanov, A.S. Melnikov, P.Y. Serdobintsev, T.A. Pakkanen, Organometallics 28 (2009) 1369–1376.
[45] I.S. Krytchankou, D.V. Krupenya, A.J. Karttunen, S.P. Tunik, T.A. Pakkanen, P.T. Chou, I.O. Koshevoy, Dalton Trans. 43 (2014) 3383–3394.
[46] T.C.W. Mak, L. Zhao, Chem. Asian J. 2 (2007) 456–467.
[47] T. Hu, L. Zhao, T.C.W. Mak, Organometallics 31 (2012) 7539–7547.
[48] T.L. Zhang, J.X. Kong, Y.J. Hu, X.G. Meng, H.B. Yin, D.S. Hu, C.P. Ji, Inorg. Chem. 47 (2008) 3144–3149.
[49] L. Zhao, T.C.W. Mak, Inorg. Chem. 48 (2009) 6480–6489.
[50] Y. Zhao, P. Zhang, B. Li, X.G. Meng, T.L. Zhang, Inorg. Chem. 50 (2011) 9097–9105.
[51] N.T. Lucas, M.P. Cifuentes, L.T. Nguyen, M.G. Humphrey, J. Cluster Sci. 12 (2001) 201–221.
[52] A.X.S. Brüker, APEX2 v2009, Madison, WI, 2009.
[53] G.M. Sheldrick, SADABS, 2008/1, University of Göttingen, Göttingen, Germany, 2008.
[54] G.M. Sheldrick, Acta Cryst. A46 (1990) 467–473.
[55] G.M. Sheldrick, Acta Cryst. A64 (2008) 112–122.
[56] H. Schmidbaur, A. Schier, Angew. Chem. Int. Ed. 54 (2015) 746–784.